Intelligent layout design of building damping structure based on ramp model

Xinjun Wang

School of Urban Construction,
Chengdu Polytechnic,
Shuangliu District, Chengdu City, China
Email: maolv505@126.com

Abstract: The increasing frequency of earthquakes has had a significant impact on citizens' property and life safety. In order to reduce the losses caused by earthquakes, the research is conducted from the perspective of structural layout of building shock absorption. This paper realises the synchronous optimisation of the layout position and damping coefficient of viscous fluid dampers under the actual ground motion. The ramp model in the density method of structural topology optimisation is used to continuously process the discrete design variables in the objective function of the optimisation problem, and then the moving asymptote method is used to solve the optimisation problem. The results show that different damper groups will lead to great differences in project cost; when a single type of damper is selected to participate in the layout optimisation, the required total damping coefficient is 23,020 k $Nm^{-1}s$. When two types of dampers are used to participate in the layout optimisation, the required total damping coefficient is 20,550.8 k $Nm^{-1}s$. The cost of a single group of dampers is significantly higher than that of two groups of dampers.

Keywords: building shock absorption; damper layout; damper coefficient; structural cost; ramp model; synchronous optimisation.

Reference to this paper should be made as follows: Wang, X. (2023) 'Intelligent layout design of building damping structure based on ramp model', *Int. J. Wireless and Mobile Computing*, Vol. 24, No. 1, pp.48–57.

Biographical notes: Xinjun Wang is an Associate Professor with the School of Urban Construction Chengdu Polytechnic, Chengdu, China. She received the BS degree in 2004 and the MS degree in 2007 from Chongqing University, China. Her research interests include structural engineering, structural earthquake resistance and intelligent construction technology.

1 Introduction

Many cities in China are in areas where earthquakes frequently occur. As a sudden and highly destructive natural disaster, earthquakes are bound to bring huge casualties and economic losses to the society. There are two methods to realise the vibration control of building structure. The first is to adjust the relevant parameters such as mass, stiffness and damping of the structure to improve its dynamic performance (Ma et al., 2021). The other is to resist earthquake action through external resistance by applying external energy. The arrangement of additional dampers in the structure for earthquake resistance and disaster reduction belongs to one of the passive controls in structural vibration control. Passive control refers to further changing the dynamic characteristics of the structure through additional subsystems or some damping devices in the structure (Salimzadeh et al., 2020). The main methods of passive control are foundation isolation technology, energy dissipation technology and mass tuning technology. Passive control method does not need external energy input, with low cost, simple structure and easy maintenance. Therefore, it has attracted much attention and has become the most widely used control means in the engineering field (Ma et al., 2020). Combined with the previous research results, from the perspective of feasibility and engineering practice, this paper synchronously optimises the layout and damping coefficient of additional dampers for plane building structures and spatial building structures. Zhou et al. (2019) made the engineering community make full use of the damping device, analysed the characteristic equation of the system theoretically based on the transfer matrix method and calculated the cable damping and frequency of the damper by solving the equation. The results of calculation and analysis are almost the same as the results of damping and frequency obtained from the test (Zhou et al., 2019). Li et al. (2019) improved the design of eddy current damper and electromagnetic damper to improve their damping density. Through the structural design and experimental results of the new damper, it is obtained that the damping density of the new damper is at the same level as that of VFD and there is no fluid leakage (Li et al., 2019). Noruzvand et al. (2021) proposed a new method to determine the constant used to correct the FVD damping coefficient, so that the ddbd model does not need to be iterated. Its performance is compared and verified by simulated seismic records. The experimental results show that the proposed method records the design performance level in different seismic effects. From the perspective of design method and bending performance, the performance of this method is more excellent (Noruzvand et al., 2021). Aiming at the discrete design variables in the objective function, combined with the density method of topology optimisation in topology optimisation, the mixed integer programming problem is transformed into a continuous problem, which is solved by moving asymptote method, which reduces the difficulty of solution. Under the premise of safety of the structure under earthquake, the goal of the lowest cost of damper layout is achieved.

Firstly, the optimisation model ramp of viscous damper of building structure is established, and the layout and damping coefficient of plane structure and spatial structure are optimised synchronously by limiting the relative storey displacement of frame building structure. Then through experiments, the optimised results are compared and analysed. Finally, the optimisation results of ramp model are summarised and the deficiencies in the research are analysed.

2 Layout and damping coefficient optimisation of building damping structures based on RAMP model

2.1 *Topology optimisation method model of viscous damper for building structure*

The energy dissipation mechanism of viscous damper is that under the action of ground motion, the viscous medium in the damper and the components of the damper act continuously to dissipate the energy transmitted from the structure to the damper, so as to ensure that the structure will not be damaged. Viscous damper is widely used in engineering because of its small shape and size, low-temperature sensitivity, large output force and high durability and reliability (Issa et al., 2020). In general, viscous dampers cannot increase the stiffness of the structure, but if more dampers are arranged in the structure, the overall stiffness of the structure will be reduced due to the lack of load-bearing members. For this, the topology layout of the damper can be optimised in combination with Solid Isotropic Material with Penalisation (SIMP). Its advantage is that it not only artificially reduces the complexity of homogenisation, but also improves the convergence of 0–1 solution (Lamichhane et al., 2021). In simp model, the relationship between density design variables and material properties is shown in formula (1).

$$E(\rho_i) = g(\rho_i)E_0 = \rho_i^p E_0,\ g(\rho_i) = \rho_i^p \tag{1}$$

In formula (1), p represents the penalty factor, E_0 represents the young's modulus of the material, for flexibility targets, $p > 1$ affects the density, making the results tend to 0–1 solutions. p too low or too high will lead to too many greyscale or too fast convergence to the local minimum; Experience shows that $p = 3$ can ensure good convergence to the solution close to 0–1. The Rational Approval of Material Properties (RAMP) model is close to the SIMP model, and the function expression is shown in formula (2).

$$E(\rho_i) = \frac{\rho_i}{1+q(1-\rho_i)}E_0,\ g(\rho_i) = \frac{\rho_i}{1+q(1-\rho_i)} \tag{2}$$

In formula (2), p and q represent the penalty factor, the difference between SIMP and RAMP is that the latter has a non-zero gradient for $\rho_i = 0$, which may affect the convergence characteristics and may alleviate the pseudo low density situation in dynamic problems. It should be noted that the choice of penalty factor mostly depends on the actual problem and is not unique (Fernandes et al., 2021). In the case of minimising flexibility, the parameters of SIMP and RAMP need to be adjusted in order to obtain sufficient penalty. The problem to be solved in this paper is the optimal layout, model and size of additional dampers in building structures (Fahiminia and Shishegaran et al., 2020). Therefore, the number of possible locations of dampers and the number of damper model groups to be considered will lead to a large number of discrete design variables. In order to effectively solve this problem, we need to learn from the idea of material interpolation in topology optimisation.

2.2 *Synchronous optimisation of damper layout and damping coefficient of plane structure*

In this paper, by limiting the relative storey displacement of frame building structure, the synchronous optimisation of damper layout position and damping coefficient is carried out, so as to achieve the purpose of minimising the project cost under the structural safety standard (Li et al., 2021). The column expression of synchronous optimisation problem is shown in formula (3).

$$\min J \quad s.t. d_c \le d_{\max} \quad 0 \le c_d \le c_{\max} \tag{3}$$

In formula (3), J is the engineering cost of the viscous damper selected in the engineering optimisation problem, which is the objective function of the optimisation problem. The damping coefficient is expressed in c_d, and each damper is used to characterise its energy dissipation capacity. In this paper, the engineering cost of a single viscous damper is regarded as its damping coefficient is positively correlated. In practical engineering, many types of dampers are often used for structural damping optimisation, which can play a more economic effect (Yaghmaei-Sabegh et al., n.d.). In the above optimisation problem, the project cost depends on the number of dampers used in each group. Therefore, the expression of the project cost and the damping coefficient of the *j*-th layer damper is obtained. See formula (4) for details.

$$J = \sum\nolimits_n^m N_n c_n \quad c_{d,j} = \sum\nolimits_{n=1}^m x_{jn} c_n \tag{4}$$

In formula (4), m represents the number of groups of dampers selected; N_n represents the number of dampers in group *n*; c_n represents the damping coefficient of group n damper; The variable x_{jn} represents the damper of the *n*-th model group present in position *J*. According to the requirements of structural optimisation design, the optimal objective function is obtained by changing the value of design variables under limited conditions. The optimisation problem should ensure that only one type of damper can be arranged on each floor of the structure. The damage caused by earthquake to the structure is divided into structural damage and non-structural damage (Wang et al., 2020). The response parameters obtained from the dynamic analysis of the structure can be used to judge the damage process of the structure. In this paper, the maximum relative displacement between floors is limited as the standard to judge whether the structure is safe. See formula (5) for its mathematical expression.

$$d_c = \max_t \left(\left| \left[D\left(d_{all}\right) \right]^{-1} Hu(t) \right| \right) \tag{5}$$

In formula (5), d_c represents the normalised value of the maximum relative interlayer displacement, H represents the conversion matrix and d_{all} represents the maximum allowable value of the relative interlayer displacement. Since the maximum relative horizon displacement $u(t)$ is normalised by the maximum allowable value, the maximum value of d_c is 1. When $d_c < 1$, it indicates that the structure is safe under the action of ground motion. Based on the application of RAMP model in the field of topology optimisation, this paper deals with the discrete design variables in the objective function to make it continuous (Noruzvand et al., 2021). The penalty coefficient can make the density close to 1 or 0, and then indicate the presence or absence of material at the location of the unit. In this paper, discrete design variables are processed continuously. See formula (6) for details.

$$x_i = \frac{x_{i,j}}{1 + p\left(1 - x_{i,j}\right)} \tag{6}$$

In formula (6), the penalty coefficient p can also make the value of x_i tend to 1 or 0, and the discrete design variables expressed in continuous form are obtained, which can improve the calculation efficiency. After the continuous processing, x_i is in the interval [0, 1]. Extract the equivalent damping coefficient $\overline{c}_d$ from another kind of design variable of the objective function to obtain a new design variable y, whose value range is also in the interval [0, 1]. See formula (7) for the new objective function.

$$J\left(x, y\right) = \overline{c}_d x_1^T \left\{ y_1 1 - x_2 y_1 + x_2^T \left[y_2 1 + \left(y_3 - y_2\right) x_3 \right] \right\} \tag{7}$$

In formula (7), In formula (7), the damping coefficients of the three model groups, c_1, c_2, c_3 are determined by y_1, y_2, y_3 respectively, $c_i = \overline{c}_d y_i$, x_k is used to determine the layout position of the damper, and its value is 0 or 1. The value range of the two types of design variables in the objective function is unified, and the complexity of programming is greatly reduced. In this paper, deterministic seismic wave records are used to analyse the dynamic response of the structure, and the records that have the greatest damage to the structure are found from the seismic wave set. The seismic wave set selected in this example is 'medium earthquake records with a recurrence period of 50 years' recorded as La series seismic set (Toosy et al., 2021), as shown in Table 1.

Table 1 Records of moderate earthquakes with a recurrence period of 50 years

Number	*Seismic wave record*	*PGA (cm/sec^2)*	*Duration (s)*	*Distance from fault (km)*
LA01	Imperial Valley,1940, El Centro	452.03	39.38	10
LA02	Imperial Valley,1940, El Centro	662.88	39.38	10
LA03	Imperial Valley, 1979, Array#05	386.04	39.38	4.1
LA04	Imperial Valley, 1979, Array#05	478.65	39.38	4.1
LA05	Imperial Valley, 1979, Array#05	295.69	39.38	1.2
LA06	Imperial Valley, 1979, Array#05	230.08	39.38	1.2
LA07	Landers, 1992, Barstow	412.98	79.98	36
LA08	Landers, 1992, Barstow	417.49	79.98	36
LA09	Landers, 1992, Yermo	509.7	79.98	25
LA10	Landers, 1992, Yermo	353.35	79.98	25
LA11	Loma Prieta, 1989, Gilroy	652.49	39.98	12
LA12	Loma Prieta, 1989, Gilroy	950.93	39.98	12
LA13	Northbridge, 1994, Nwehall	664.93	59.98	6.7
LA14	Northbridge, 1994, Nwehall	644.49	59.98	6.7
LA15	Northbridge, 1994, Rinaldi RS	253.3	14.945	7.5
LA16	Northbridge, 1994, Rinaldi RS	568.58	14.945	7.5
LA17	Northbridge, 1994, Sylmar	558.43	59.98	6.4
LA18	Northbridge, 1994, Sylmar	801.44	59.98	6.4
LA19	North Palm Spring, 1986	999.43	59.98	6.7
LA20	North Palm Spring, 1986	967.61	59.98	6.7

The selection of seismic wave requires dynamic analysis of the structure without additional damping, so as to find out the ground motion record that causes the greatest damage to the structure. The starting of the moving asymptote method needs to give the initial value of the design variable, and the sensitivity is solved by the finite difference method in the iterative process. The number of selected viscous fluid damper model groups needs to be determined in advance. Combined with the number of structural floors, the number of optimisation design variables can be determined. The remaining parameters are determined according to engineering experience (Khalifa et al., 2020). Assuming that the damper damping coefficients at all positions in the initial iteration step are the same, determine the values of the initial design variables X and y as the starting point of the optimisation iteration, determine the judgment criterion of iteration convergence, and start the optimisation iteration.

2.3 *Synchronous optimisation of damper layout and damping coefficient of spatial structure*

For linear plane frame structures, the layout of additional dampers and the simultaneous optimisation of damper coefficients are carried out, and the optimal layout of viscous fluid dampers in plane shear frame structures under ground motion is obtained. In engineering practice, the structure is often a complex spatial structure with a large number of nodes, which needs to take into account the bending and torsion of components under load. Therefore, it is also necessary to optimise the layout of viscous fluid dampers of spatial linear building structures (Wu et al., 2020). Among them, the spatial linear main structure analysis model is shown in Figure 1.

Engineering structures are actually spatial systems, and some spatial structures can be transformed into plane structures for calculation under specific conditions. In the optimisation problem of this paper, a big difference between spatial structure and plane structure is that the torsional effect of spatial structure can consume part of energy, which belongs to an attribute of the structure itself to resist external load. This attribute can reduce the amount of damper for the optimisation problem of this paper. Owing to the characteristics of many nodes and degrees of freedom, the calculation amount of damper layout optimisation of space building structure is significantly greater than that of plane simplified model (Wei et al., 2020). In this paper, the layout position and damping coefficient optimisation of viscous dampers in linear space structures will be analysed. The member system model will be the main analysis model of the spatial structure in this paper. The model takes beams, columns and other members as the basic elements, focuses the structural mass on each node for calculation and uses the member restoring force model to represent the change relationship of element stiffness with internal force (Li et al., 2020). In the example part of this paper, when analysing the spatial building structure, the component element in the structure is regarded as the spatial beam element and the node force of the spatial beam element is shown in Figure 2.

Figure 1 Schematic diagram of spatial linear main structure analysis model

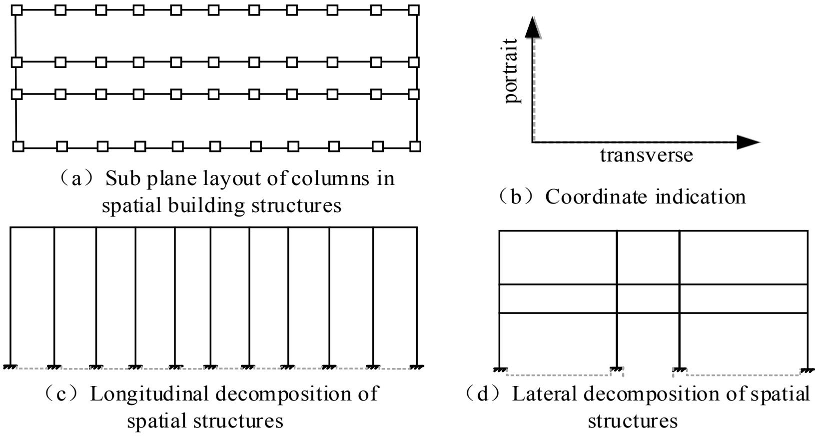

Figure 2 Nodal force of spatial beam elements

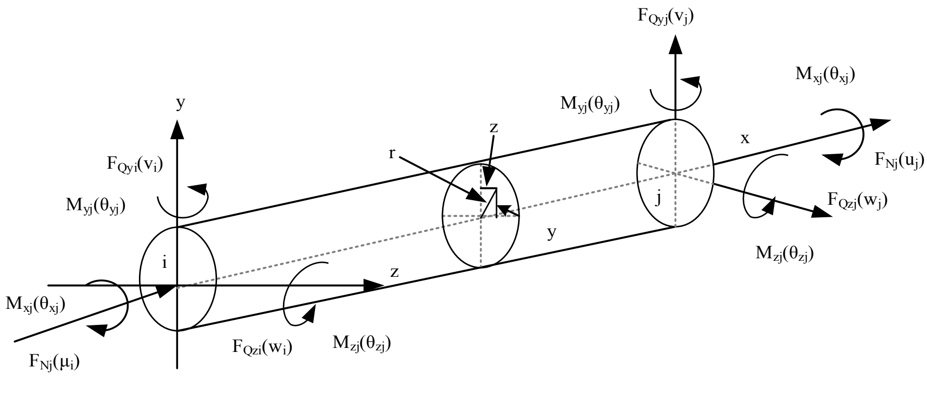

As shown in Figure 2, the load action direction of the spatial beam element is in a different plane from the main axis of the beam element section. For the spatial beam element, it is assumed that each node has six displacement degrees of freedom and six node forces correspond to it, respectively. For the beam element with numbers *i* and *j* at both ends in the structure, the coordinate system in the figure is the right-hand coordinate system, and the axis direction of the member element is the *X*-axis. The principal axes of inertia of the section are *Y*-axis and *z*-axis, respectively. See formula (8) for the function expression of node displacement vector $\delta_i \delta_j$.

$$\begin{cases} \delta_i = \left[u_i \ v_i \ w_i \ \theta_{xi} \ \theta_{yi} \ \theta_{zi} \right]^T \\ \delta_j = \left[u_j \ v_j \ w_j \ \theta_{xj} \ \theta_{yj} \ \theta_{zj} \right]^T \end{cases} \tag{8}$$

In formula (8), u represents torsional displacement, θ_x represents torsional angle, v and w represent deflection. The function expression of the corresponding node vector $f_i f_j$ is shown in formula (9).

$$\begin{cases} f_i = \left[F_{Ni} \ F_{Qyi} \ F_{Qzi} \ M_{xi} \ M_{yi} \ M_{zi} \right]^T \\ f_j = \left[F_{Nj} \ F_{Qyj} \ F_{Qzj} \ M_{xj} \ M_{yj} \ M_{zj} \right]^T \end{cases} \tag{9}$$

In formula (9), F_{Ni}, F_{Nj} represent the axial forces at nodes *i* and *j*, respectively; And $F_{Qyi}\ F_{Qzi}$, $F_{Qyj}\ F_{Qzj}$ represents the shear along the two main inertia axes, respectively; M_{xi}, M_{xj} represents the torque to the *x*-axis; $M_{yi}\ M_{zi}$, $M_{yj}\ M_{zj}$ represents the bending moment around the main inertia axis respectively. After a series of derivation, the total stiffness matrix, total mass matrix and total damping matrix of spatial structure are finally obtained (Krish et al., n.d.).

3 Analysis of optimisation results of shock absorption structure layout and damping coefficient of RAMP model building

3.1 Synchronous optimisation results of damper layout and damping coefficient of plane structure

The seismic wave set selected in this example is 'moderate earthquake records with a recurrence period of 50 years'. The selection of seismic wave requires the dynamic analysis of the structure without additional damping. The optimised iteration stop conditions are as follows: the change of design variable value in two iterative analysis steps is less than $1e^{-3}$; The normalised displacement constraint value is less than a set value. The example is a two-storey shear frame structure, and the mass of each layer of the structure is M1 = 25,000 kg and M2 = 25,000 kg, respectively; The stiffness of each layer of the structure is K1 = 37,500 kN / m and K2 = 25,000 kN/ m, respectively. Among them, the time history results of la02 seismic wave acceleration are shown in Figure 3.

It can be seen from Figure 3 that the dynamic analysis of the double-layer shear structure without additional damper shows that under the value of arbitrary damping ratio, the floor displacement of the structure is the largest under the action of ground motion LA02, so the ground motion record LA02 has the strongest seismic damage to the structure. The layout optimisation results of dampers for two-story shear frame structure are shown in Table 2.

Figure 3 Acceleration time history of LA02 seismic wave

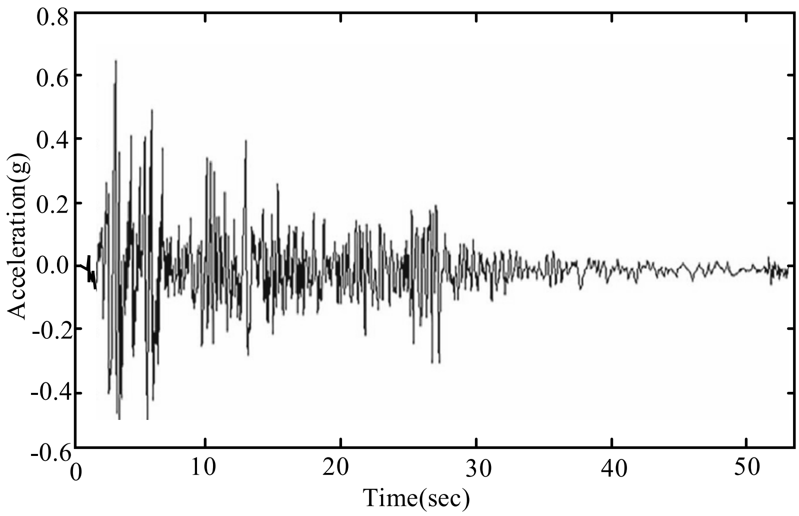

Table 2 Layout optimisation results of single group and two groups of dampers

Numerical example	*Location*	*x*	C_d	*Selected damper*
Example 1	1	0.9973	1123.2	1120.2
	2	0.9934	1127.6	1120.2
				∑=2240.4
Example 2	1	0.9949	1.2697e+003	1.2632e+003
	2	0.9979	0.1821e+003	0.1766e+003
				∑=1.4398e+003

It can be seen from Table 2 that the damper with a parameter of 1120.2 kNm^{-1}s is used at both positions of a single group of dampers, which can achieve the lowest project cost on the premise of ensuring safety. At the same time, to ensure the same structural parameters and ground motion records, as well as the same optimisation parameters, two groups of dampers are selected to participate in the optimisation and the number of design variables is 6, the two groups of damper layout optimisation structure can be obtained. It can be seen from the optimisation results that under the action of ground motion LA02, the damping coefficient of the two-storey shear structure is 1263.2 kNm^{-1}s on the first floor and 176.6 kNm^{-1}s on the second floor, which can ensure the safety of the structure and achieve the optimal engineering cost. The convergence image of the optimisation iteration of the two groups of damper structures is shown in Figure 4.

It can be seen from Figure 4 that the difference between the two figures lies in the different initial points of iteration. The black curve in the figure is the contour of constraint function and the black dotted line is the contour of objective function. It can also be seen from Figure 4 that the constraint is convex, indicating that the local optimal solution of the problem is the global optimal solution. It is concluded that under the same structure and the same parameters, different damper groups will lead to great differences in project cost.

3.2 Synchronous optimisation results of damper layout and damping coefficient of spatial structure

The calculation example adopts a five story three span symmetrical spatial structure with three displacement degrees of freedom at each node. The structure has a total of 48 nodes and 144 displacement degrees of freedom. Assuming that the damping of the first two modes is 5% structural Rayleigh damping, there are 10 locations where dampers can be arranged. Based on the premise that the damper model of each layer is the same, a single group of dampers participate in the synchronous optimisation of layout and damping coefficient, The number of design variables is 6, the initial value of design variables is $X_i = 0.5(I = 1, 2, ..., 5)$, y = 1. Among them, the schematic diagram of 5-storey 3-span symmetrical spatial structure is shown in Figure 5.

Figure 4 Convergence image of optimisation iteration of two groups of damper structures

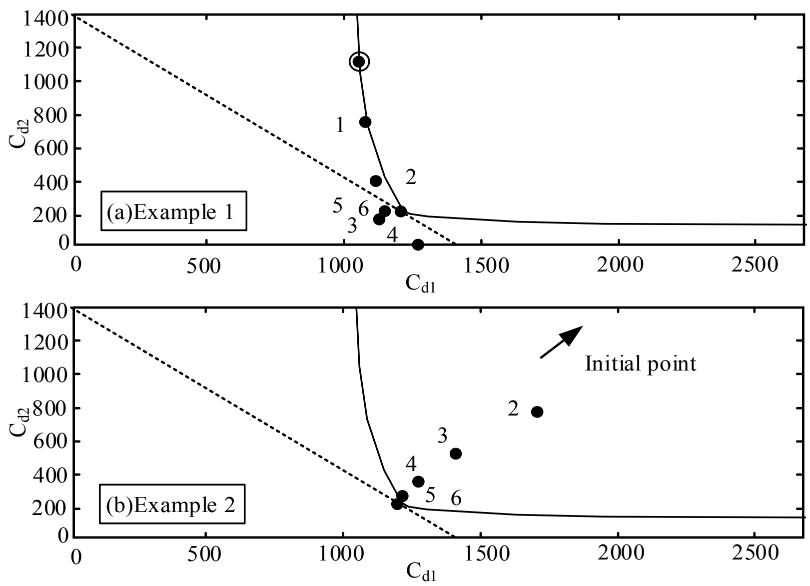

Figure 5 Is a schematic diagram of a 5-storey 3-span symmetrical spatial structure

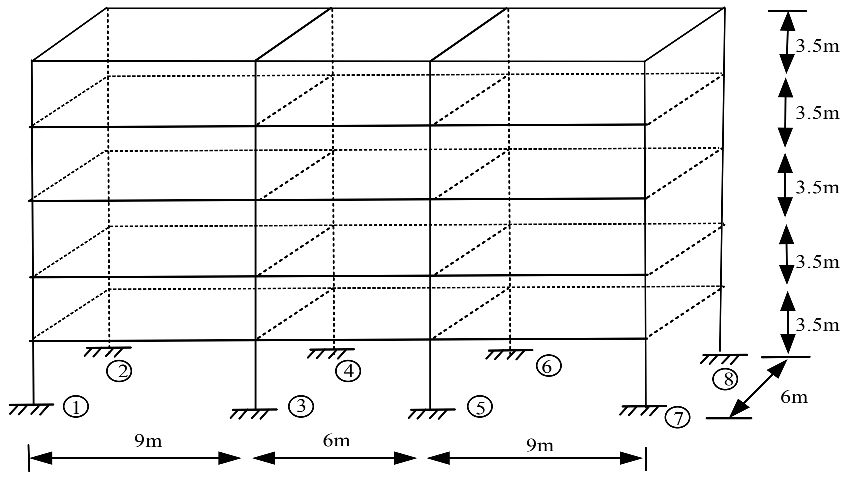

In Figure 5, the dimensions of columns numbered 1, 2, 7 and 8 are 0.7 m × 0.7 m, the size of columns numbered 3, 4, 5 and 6 is 0.5 m × 0.5 m, beam size is 0.4 m × 0.6 m, material Young's modulus E = 25.5 Gpa, material density is determined as 2500 kg / m^3, and the maximum allowable value of relative interlayer displacement D_{all} is 1% of storey height, d_c = 15,000 k Nm^{-1}s. There are six design variables when a single group of dampers participate in the optimisation of the structure. Among them, the structural response results of the example under different seismic waves are shown in Figure 6.

Figure 6 shows the maximum floor displacement of the structure under different damping ratios. The index value of the maximum floor displacement represents the destructive effect of the earthquake on the structure. It can be seen from the image that under the value of arbitrary damping ratio, the displacement value of the frame building structure is the largest under the action of LA16, so LA16 is the most destructive to the structure. Among them, the damping coefficients of viscous dampers arranged on each floor before and after iterative optimisation of single group and biped dampers are shown in Figure 7.

It can be seen from Figures 7(a) and 7(b) that under the action of LA16 ground motion recording, a damper with a damping coefficient of 11510.0 kNm^{-1}s needs to be arranged at the corresponding position of the second floor of the structure, which can ensure the safety of the structure and optimise the project cost. It can be seen from Figures 7(c) and 7(d) that under the action of LA16 ground motion recording, the double group damper structure needs to arrange dampers with damping coefficients of 9134.8 kNm^{-1}s and 1140.6 kNm^{-1}s, respectively at the corresponding positions of the second and fourth floors of the structure, which can ensure the safety of the structure and optimise the project cost.

Through the comparison of single and double group dampers, it is found that when there are more choices of structural damper models, the total damping coefficient required will be reduced, and the project cost will also be reduced. Therefore, an eight storey 3×3 building with symmetrical spatial structure is selected for calculation. Select the three views of the structure of the building, as shown in Figure 8. In the three views of Figure 8, the structural nodes have three degrees of freedom of displacement. The damping value of the first two node modes is set as 5% structural Rayleigh damping. The la07 with the most serious damage to the structure is selected for seismic waves, and three groups of dampers are used to participate in the synchronous optimisation of the layout and damping coefficient of the building.

Figure 6 Structural response under different seismic waves

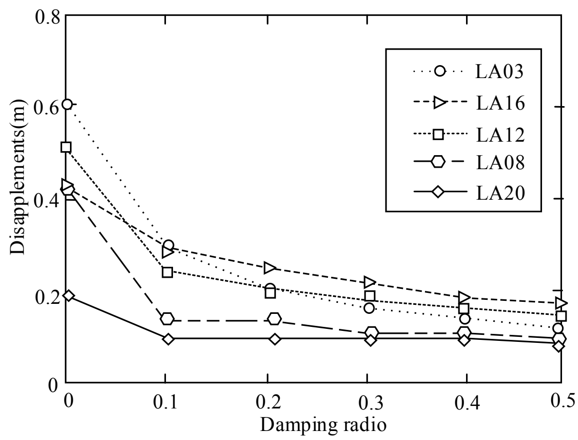

Figure 7 Damping coefficients of viscous dampers arranged on each floor before and after iterative optimisation of single group and biped dampers

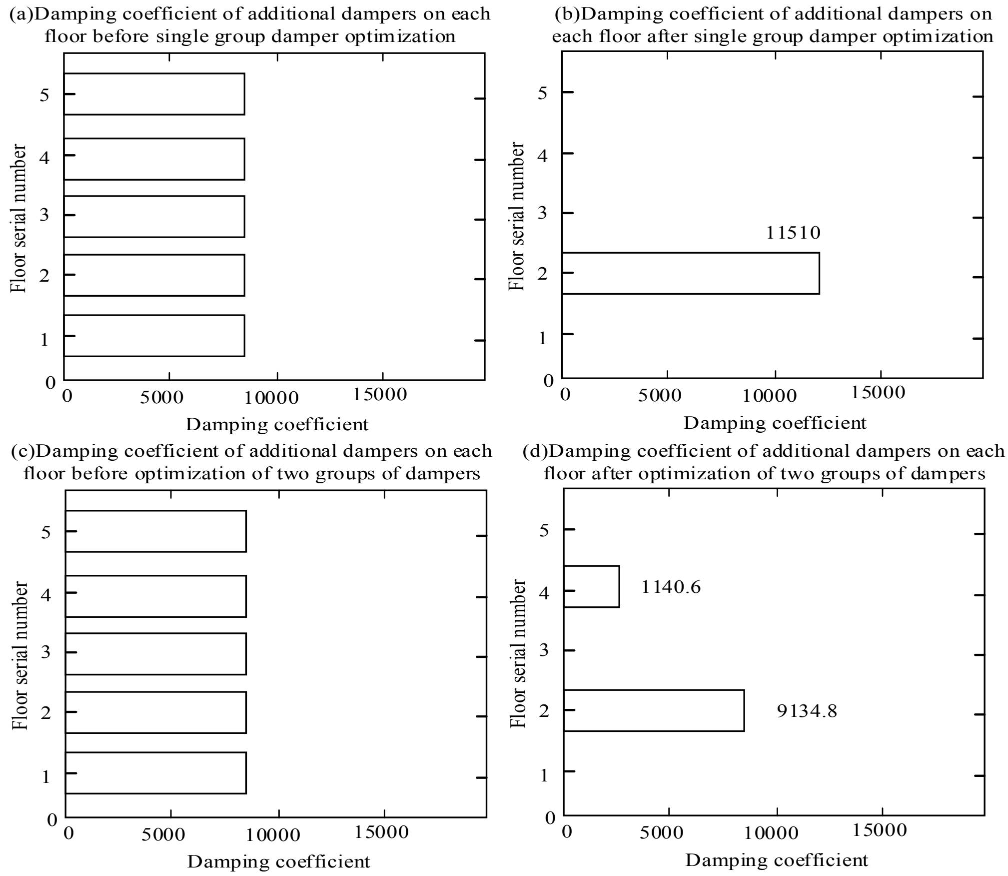

Figure 8 Example 3 building three view structure

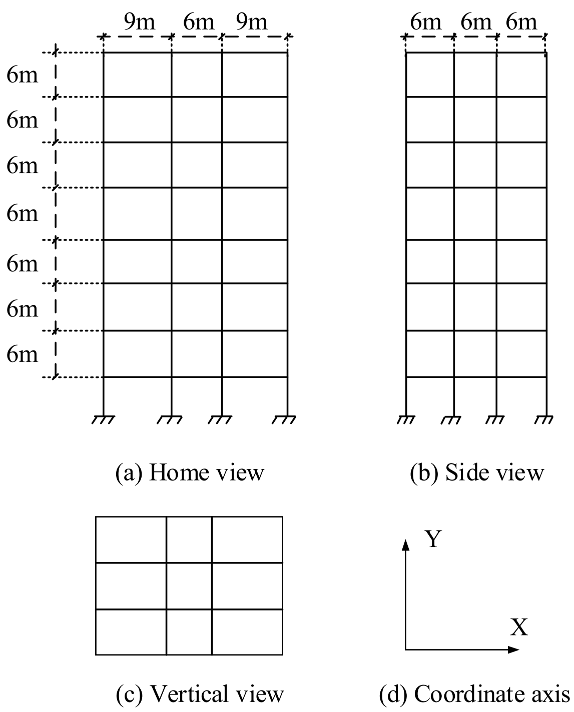

Three views of building structure

In Figure 8(a), the dimensions of the three spans of the building are 9, 6 and 9 m, respectively. From Figure 8(b), it can be seen that the dimensions of the three spans in the side view are 6 m, the height of each floor of the building structure is 3.5 m, the length and width of the columns are 0.7 m, the dimensions of the beams are 0.5m, the young's modulus of the material is $E = 25.5\,\text{GPa}$, the material density is set to $2500\,\text{kg/m}^3$ and the maximum allowable value of the relative storey displacement is 1% of the floor height, that is $D_{\text{all}} = 0.01\text{h}$, $\overline{c}_d = 20000\,\text{kNm}^{-1}\text{s}$, Among the three groups of dampers, 27 design variables are optimised. The acceleration time history recorded by the ground motion and the final layout optimisation of the viscous damper are shown in Figure 9.

According to the ground motion records in Figure 9(a), the damping coefficients of dampers arranged at the corresponding positions of the first three floors of the building structure are $\overline{c}_d = 18809.4\,\text{kNm}^{-1}\text{s}$, $\overline{c}_d = 9009.6\,\text{kNm}^{-1}\text{s}$ and $\overline{c}_d = 7076.3\,\text{kNm}^{-1}\text{s}$, respectively. At this time, the optimised layout structure can ensure safety and reduce the project cost. Compared with single group and double group dampers, its seismic effect is better and the project cost is lower. Therefore, the damper layout is optimised to a certain extent, and its cost problem decreases with the increase of the number of damper models.

Figure 9 Acceleration time history of ground motion records and final layout optimisation of viscous dampers

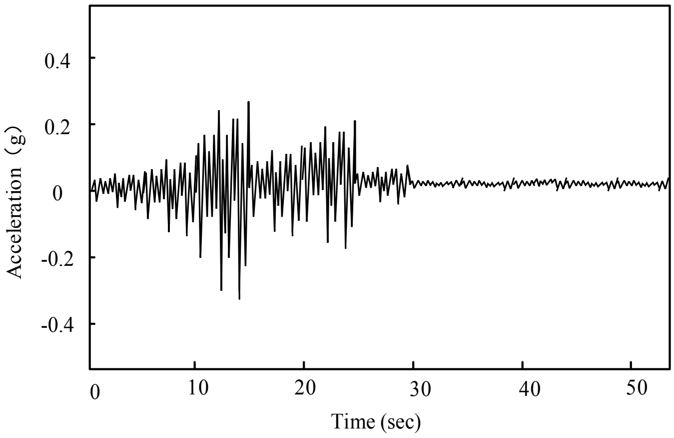

(a) La07 seismic wave acceleration time history

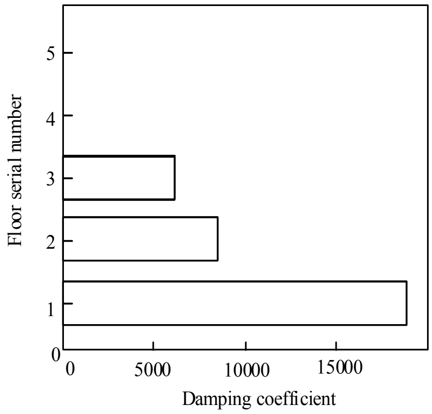

(b) Damping coefficient of additional dampers on each floor before optimization of two groups of dampers

4 Conclusion

In order to solve the huge loss of life and property caused by earthquake, starting from the study of viscous dampers in buildings, a method of reasonable layout and optimal selection of viscous dampers is proposed. Combined with the actual engineering background, the cost of engineering optimisation problem is combined with the cost related to the structure, model and prototype test of dampers, which is taken as the objective function of the optimisation problem. The dynamic response of the structure is analysed by using deterministic ground motion records, and the peak value of relative storey displacement is taken as the constraint function of the optimisation problem. Taking the layout position and damping coefficient of viscous fluid dampers as design variables, the formulation of optimisation problem is constructed. Referring to the application of material interpolation technology in the field of topology optimisation, combined with the ramp model in the density method, the discrete design variables in the objective function are processed to make them continuous, which reduces the complexity and difficulty of solving the problem and improves the programming efficiency and calculation efficiency. At the same time, this method is also applicable to plane frame and spatial frame structures, has high calculation efficiency, and obtains the synchronous optimisation design scheme of viscous damper position layout and damping coefficient of building damping structure on the premise of minimum cost. There are still deficiencies in the research, and the optimal combination of the number of viscous damper groups has not been determined. Subsequent research will focus on this part to make the building more safe and economical.

References

Fahiminia, M. and Shishegaran, A. (2020) 'Evaluation of a developed bypass viscous damper performance', *International Journal of Frontiers of Structural and Civil Engineering*, Vol. 14, No. 6, pp.773–791

Fernandes, M., Rodrigues, S. and Sharma, S. et al (2021) 'Comparative study of seismic behaviour of high rise building with and without use of fluid viscous damper using e-tabs', *International Journal of International Journal of Innovations in Engineering and Science*, Vol. 6, No. 5, pp.22–30.

Issa, E., Issa, J. and Musa, S. et al. (2020) 'Structural efficiency of the building form for optimization the diagrid structure', *International Journal of International Journal of Advanced Science and Technology*, Vol. 29, No. 3, pp.12572–12589.

Khalifa, M., Al-Kahtan, Y.K. and Farouk, S. et al. (2020) 'Microfacies architecture and depositional history of the Upper Jurassic (kimmeridgian) Jubaila Formation in central Saudi Arabia', *International Journal of African Earth Sciences*, Vol. 174, No. 5, pp.104076–104076.

Krish, A., Streicher, J.W. and Hanson, R.K. (n.d.) 'Ultraviolet absorption cross-section measurements of shock-heated O_2 from 2000–8400 K using a Tunable Laser', *International Journal of Quantitative Spectroscopy and Radiative Transfer*, Vol. 247, No. 3, pp.106959–106959.

Lamichhane, K., Lamichhane, P.D. and Ghimire, K. et al. (2021) 'Analysis of irregular structure with addition of shear walls as per nepal building code (NBC 105:2020)', *International Journal of International Journal of Engineering and Technical Research*, Vol. 10, No. 3, pp.608–608.

Li, J.Y., Zhu, S. and Shen, J. (2019) 'Enhance the damping density of eddy current and electromagnetic dampers', *International Journal of Smart Structures and Systems*, Vol. 24, No. 1, pp.15–26.

Li, S., Xiang, P. and Wei, B. et al. (2021) 'Interface friction effects on scaling a vertical spring-viscous damper isolation system in a shaking table test', *International Journal of Structures*, Vol. 33, Nos. 4/6, pp.1878–1891.

Li, Z., Li, D. and Peng, L. et al. (2020) 'Study on the damping efficiency of continuous beam bridge with constant cross-section applied by lead rubber bearings and fluid viscous dampers', *International Journal of Noise and Vibration Worldwide*, Vol. 51, Nos. 4/5, pp.85–92.

Ma, A., Tan, P. and Wang, S. et al. (2020) 'Stochastic optimization of continuous beam bridge viscous damper considering the fluid-solid coupling effect and its damping performance', *International Journal of International Journal of Heat and Technology*, Vol. 38, No. 1, pp.37–37.

Ma, G., Wang, Y. and Jiang, S. (2021) 'Optimization of building exit layout: combining exit decisions of evacuees', *International Journal of Advances in Civil Engineering*, No. 1, pp.1–16.

Noruzvand, M., Mohebbi, M. and Shakeri, K. (2021) 'An improvement of direct displacement-based design approach for steel moment-resisting frames controlled by fluid viscous dampers', *International Journal of Advances in Structural Engineering*, Vol. 24, No. 10, pp.2148–2160.

Salimzadeh, N., Vahdatikhaki, F. and Hammad, A. (2020) 'Parametric modelling and surface-specific sensitivity analysis of PV module layout on building skin using BIM', *International Journal of Energy and Buildings*, Vol. 216, No. 4, pp.109953–109953.

Toosy, M., Khan, S. and Shakir, U. et al. (2021) 'Depositional architecture of eocene and cretaceous reservoirs (blending seismic and well data) in Mubarik Area, Central Indus Basin, Pakistan', *International Journal of Pure and Applied Geophysics*, Vol. 178, No. 4, pp.1297–1315.

Wang, X., Yang, J. and Wang, F. (2020) 'Novel adaptive tuned viscous inertance damper (ATVID) with adjustable inertance and damping for structural vibration control', *International Journal of Structures*, Vol. 29, No. 1, pp.814–822.

Wei, T., Chen, Z. and Li, P. et al. (2020) 'Early use of endotoxin absorption by oXiris in abdominal septic shock: a case report', *International Journal of Medicine*, Vol. 99, No. 28, pp.e19632–e19632.

Wu, J.Z., Pan, C.S. and Ronaghi, M. et al. (2020) 'Application of air-bubble cushioning to improve the shock absorption performance of type I industrial helmets', *International Journal of Engineering Failure Analysis*, Vol. 117, No. 11, pp.104921–104921.

Yaghmaei-Sabegh, S., Jafari-Koucheh, E. and Ebrahimi-Aghabagher, M. (n.d.) 'Estimating the seismic response of nonlinear structures equipped with nonlinear viscous damper subjected to pulse-like ground records', *International Journal of Structures*, Vol. 28, No. 6, pp.1915–1923.

Zhou, H.J., Yang, X. and Pang, Y.R. et al. (2019) 'Damping and frequency of twin-cables with a cross-link and a viscous damper', *International Journal of Smart Structures and Systems*, Vol. 23, No. 6, pp.669–682.